J. Fluid Mech. (1969), *vol.* 36, *part* 4, *pp.* 735–757
Printed in Great Britain

Lifting-surface theory for cascade of blades in subsonic shear flow

By MASANOBU NAMBA

Department of Aeronautical Engineering,
Kyushu University, Fukuoka, Japan

(Received 24 July 1968)

A lifting-surface theory is presented for a cascade in subsonic shear flow by applying Fourier integral methods to the expressions of the perturbed flow field. The pressure distribution on the blade surface is determined by means of the so-called singularity method. Some numerical examples are presented and discussed in comparison with the results according to the lifting-line theory.

A significant difference is found in the effect of compressibility between a shear flow and a uniform flow. In shear flows with the maximum Mach number close to one, no such great local lift force is found near the sonic station as would be predicted by the linearized subsonic uniform flow theory. The correlation between the local lift and the local effective angle of attack at high Mach number span-stations shows a great deviation from that according to the uniform flow theory.

1. Introduction

In recent years considerable effort has been devoted to improve the thrust/weight ratio of aircraft gas turbine engines. In order to meet such a requirement it is desirable to increase the inlet Mach number relative to the compressor rotor. Therefore it is of much importance to know the compressor performance in high Mach number levels. The flow in the turbomachines is known to be essentially three-dimensional from various sources. Especially when we have to deal with high-speed flow and take into account the compressibility effect, it should be emphasized that the relative Mach number is in general non-uniform along the blade span.

As is well known, for example from the problems of axisymmetric flow, the effect of compressibility in three-dimensional flow is considerably different from that in two-dimensional flow. Hence theories and experiments for two-dimensional cascades would be of doubtful validity in evaluating the compressibility effect on the high Mach number internal flow in the turbomachines.

The author and his colleague conducted an experimental study (Namba & Asanuma 1965) on the linear cascade in subsonic or transonic shear flows. They have also developed a lifting-line theory for a cascade of blades in subsonic shear flow (Namba & Asanuma 1967, to be referred to hereafter as L). From these works it has been revealed that the average effect of compressibility in shear flow is closely associated with the so-called 'harmonic mean Mach number' and that

the lift distribution can be evaluated fairly well by the lifting-line theory as long as the harmonic mean Mach number is below a certain value.

However the lifting-line theory, though it takes into account the non-uniform downwash distribution along the span, assumes the effect of the Mach number upon the lift force to be similar locally at each span-station to that in two-dimensional flow. In other words the lifting-line theory is a quasi-two-dimensional theory as regards the effect of compressibility. Therefore, if the Prandtl–Glauert rule is applied to this theory, the span-stations attacked by Mach numbers very close to unity would be expected to show great lift forces. On the other hand, if we apply the experimental results in uniform flows to the assumption in this theory, then the near-sonic span-stations would suffer from stall phenomena with a significant drop of the lift force.

The author's experiments (1965 or briefly reported also in L), however, give little evidence to support either of these views. According to the experiments, the near-sonic station shows neither such a great lift force as that due to the two-dimensional Prandtl–Glauert rule nor such a stall-like pressure distribution as would be expected from the experimental results in uniform flows. In these cases the static pressure distribution on the blade surface shows a sound pattern over the whole span similar to that in the uniform flow with the Mach number corresponding to the harmonic mean Mach number of the shear flow.

In view of the experimental information stated above it can be suggested that a more complete three-dimensional theory such as a lifting-surface theory is needed for the reasonable estimation of the compressibility effect for high subsonic or transonic shear flow. Besides it may also be suggested that linearization based on the assumption of small disturbances would be practically meaningful not only in high subsonic shear flow but also in transonic shear flow.

From this aspect, a lifting-surface theory is presented in this paper for a cascade of blades in subsonic shear flow. The method of Fourier integrals used in L is extended to the representation of the disturbed flow field due to the pressure dipoles distributed on the blade surfaces. From a different standpoint, the present theory is an extension of the lifting-surface theory for incompressible shear flow given by Honda (1960, 1961) to the one for subsonic shear flow. Further developments to the transonic flow régime will appear in following papers.

2. Lifting-surface theory

2.1. *Assumptions and basic equations*

As illustrated in figure 1, let a rectangular Cartesian co-ordinate system (x, y, z) be chosen so that the x-axis and the y-axis are parallel to the directions of the undisturbed stream and the blade span respectively, where x, y and z are made dimensionless by setting the chord length of the blade equal to unity. Here we shall deal with a cascade of blades spanning between two parallel walls, through which flows a shear flow with the undisturbed velocity vector of $(U(y), 0, 0)$, i.e. with the velocity varying only spanwisely. The choice of the non-dimensional co-ordinates mentioned above renders the distance λ between the walls identical with the aspect ratio of the blades. In the present theory the following assump-

tions are made: (i) the undisturbed flow is subsonic everywhere; (ii) the fluid is an inviscid and non-conducting perfect gas; (iii) the blades are thin and their angle of attack and camber are small; (iv) the flow perturbation is small, and the entropy remains constant along each streamline.

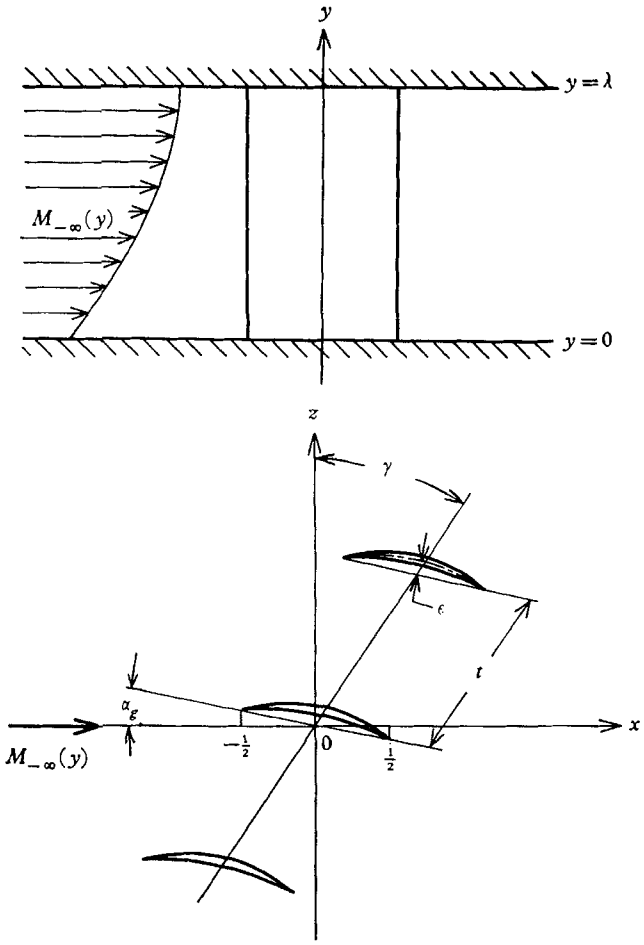

FIGURE 1. Geometry and notation of the flow model.

Let the reference pressure be the arithmetical mean of the static pressures far up- and downstream, and let p be a small perturbation of it. Then, as shown in L, from the equations of continuity, motion and energy linearized by the assumptions stated above, we get the following equation for the disturbance pressure p:

$$[1-\{M_{-\infty}(y)\}^2]\frac{\partial^2 p}{\partial x^2}+\frac{\partial^2 p}{\partial z^2}+\frac{\partial^2 p}{\partial y^2}-\frac{2}{M_{-\infty}}\frac{dM_{-\infty}}{dy}\frac{\partial p}{\partial y}=0, \tag{1}$$

where $M_{-\infty}(y)$ is the far-upstream Mach number defined by

$$M_{-\infty}(y) = U(y)/\{\kappa p_{-\infty}/\rho_{-\infty}(y)\}^{\frac{1}{2}}. \tag{2}$$

Here κ denotes the ratio of the specific heats of the fluid and $p_{-\infty}$ and $\rho_{-\infty}$ are the static pressure and the fluid density far upstream respectively. A detailed

description of the derivation of (1) is available also in Ward (1955, p. 224). In the present study, $M_{-\infty}(y) < 1$ according to assumption (i). However in order for the linearization as (1) to be justified even at the stations with the Mach number close to one, it is necessary to make an additional assumption that $|dM_{-\infty}/dy|$ is not small at the near-sonic stations.

The boundary conditions to be imposed on (1) are

$$p \to \mp \tfrac{1}{2}\Delta p \quad \text{as} \quad x \to \mp\infty, \tag{3}$$

$$\partial p/\partial y = 0 \quad \text{at} \quad y = 0, \lambda, \tag{4}$$

and

$$[w/U]_{z=mt\cos\gamma} = f(x - mt\sin\gamma) \quad \text{for} \quad |x - mt\sin\gamma| < \tfrac{1}{2} \quad (m = 0, \pm 1, \pm 2, \ldots). \tag{5}$$

Here Δp is a finite value corresponding to the increase of pressure across the cascade. The condition (4) means that the velocity component normal to the walls must vanish at the wall surfaces. Finally, (5) gives the linearized expression for the condition of tangency of the flow to the blade surfaces, where w, t and γ are the z-component of the disturbance velocity, the pitch–chord ratio and the stagger angle of the cascade respectively. Since the present analysis limits itself to the lifting problem, $f(x)$ denotes the slope of the mean camber surface of the blade. An extensive discussion of the more general problem including the thickness contribution is to be found in appendix E. Furthermore, for simplicity we shall deal with the blades with uniform geometrical configuration along the span, and hence $f(x)$ is a function of x only. However, no special difficulty would arise in solving the problem of non-uniform blade geometry, if desired.

2.2. *Expression of disturbance pressure*

As shown in L, a lifting-line can be regarded as a filament of pressure dipoles with the axes normal to the undisturbed stream. In the same way a lifting-surface can be considered as a sheet of pressure dipoles. Then extending the expression for p due to a cascade of lifting-lines given in L, we get as the solution of (1) satisfying (3) and (4) the expression for p due to a cascade of lifting-surfaces in the following Fourier integral form:

$$p = -\sum_{m=-\infty}^{\infty} \operatorname{sgn}(z - mt\cos\gamma) \int_{-\frac{1}{2}}^{\frac{1}{2}} d\xi \int_0^{\infty} \cos\{\alpha(x - \xi - mt\sin\gamma)\} \times \sum_{n=0}^{\infty} \exp(-\beta_n(\alpha)|z - mt\cos\gamma|)\, F_n(\xi;\alpha)\, Y_n(y;\alpha)\, d\alpha, \tag{6}$$

where $Y_n(y;\alpha)$ and $\beta_n(\alpha)$ are respectively the eigenfunction and the eigenvalue for the following boundary-value problem:

$$\frac{d}{dy}\left(\frac{1}{M_{-\infty}^2}\frac{dY}{dy}\right) + \left(-\frac{1 - M_{-\infty}^2}{M_{-\infty}^2}\alpha^2 + \frac{1}{M_{-\infty}^2}\beta^2\right) Y = 0, \tag{7}$$

$$dY/dy = 0 \quad \text{at} \quad y = 0, \lambda. \tag{8}$$

The eigenfunctions $Y_n(y;\alpha)$ constitute a complete set of orthogonal functions such that

$$\int_0^{\lambda} \frac{Y_n Y_m}{M_{-\infty}^2}\, dy = 0 \quad \text{for} \quad n \neq m. \tag{9}$$

As shown in L, $\{\beta_n(\alpha)\}^2$ is positive over the range of $0 < \alpha < \infty$, as long as $M_{-\infty}(y) < 1$ everywhere. Therefore $\beta_n(\alpha)$ is assured to be real over $0 < \alpha < \infty$, and the sign of $\beta_n(\alpha)$ is chosen as $\beta_n(\alpha) > 0$, in order for the condition of p vanishing at infinity to be satisfied.

The functions $F_n(x;\alpha)$ in (6) correspond to the coefficients in a series of the eigenfunctions $Y_n(y;\alpha)$ into which the pressure jump $\Delta p_s(x,y)$ across a lifting-surface is expanded. That is to say,

$$\Delta p_s(x,y) = 2\pi \sum_{n=0}^{\infty} F_n(x;\alpha)\, Y_n(y;\alpha). \tag{10}$$

Then the orthogonality of $Y_n(y;\alpha)$, (9), gives

$$F_n(x;\alpha) = \frac{1}{\lambda}\int_0^{\lambda} \frac{Y_n(y;\alpha)}{M^2_{-\infty}(y)}\,\Delta p_s(x,y)\,dy, \tag{11}$$

where the $Y_n(y;\alpha)$ are normalized by

$$\frac{1}{\lambda}\int_0^{\lambda} \frac{Y_n^2(y;\alpha)}{M^2_{-\infty}(y)} = 1. \tag{12}$$

A detailed account of the derivation of expression (6) is given in appendix D.

As shown in L, the disturbance pressure p given by (6) consists of the contribution of an isolated lifting-surface p_{I} and those of remaining ones in the cascade p_{II} and p_{III}, which can be represented in the range

$$|z| < \tfrac{1}{2}t\cos\gamma \tag{13}$$

as follows:

$$p = p_{\mathrm{I}} + p_{\mathrm{II}} + p_{\mathrm{III}}, \tag{14}$$

$$p_{\mathrm{I}} = -\operatorname{sgn} z \int_{-\frac{1}{2}}^{\frac{1}{2}} d\xi \int_0^{\infty} \cos\{\alpha(x-\xi)\} \sum_{n=0}^{\infty} \exp(-\beta_n(\alpha)|z|)\, F_n(\xi;\alpha)\, Y_n(y;\alpha)\, d\alpha \ldots, \tag{15a}$$

$$p_{\mathrm{II}} = \int_{-\frac{1}{2}}^{\frac{1}{2}} d\xi \int_0^{\infty} \cos\{\alpha(x-\xi)\} \sum_{n=0}^{\infty} C_n(\alpha) \sinh\{\beta_n(\alpha) z\}\, F_n(\xi;\alpha)\, Y_n(y;\alpha)\, d\alpha \ldots, \tag{15b}$$

$$p_{\mathrm{III}} = \int_{-\frac{1}{2}}^{\frac{1}{2}} d\xi \int_0^{\infty} \sin\{\alpha(x-\xi)\} \sum_{n=0}^{\infty} S_n(\alpha) \cosh\{\beta_n(\alpha) z\}\, F_n(\xi;\alpha)\, Y_n(y;\alpha)\, d\alpha \ldots, \tag{15c}$$

where

$$C_n(\alpha) = \frac{\sinh\{\beta_n(\alpha)\, t\cos\gamma\}}{\cosh\{\beta_n(\alpha)\, t\cos\gamma\} - \cos(\alpha t\sin\gamma)} - 1, \tag{16}$$

$$S_n(\alpha) = \frac{\sin(\alpha t\sin\gamma)}{\cosh\{\beta_n(\alpha)\, t\cos\gamma\} - \cos(\alpha t\sin\gamma)}. \tag{17}$$

Once the coefficients $F_n(x;0)$ are determined, by the method shown later, then the pressure jump across the blades can be calculated by

$$\Delta p_s = 2\pi \sum_{n=0}^{\infty} F_n(x;0)\, Y_n(y;0) \tag{10a}$$

and hence the pressure jump coefficient across the blades is given by

$$\begin{aligned} C_p &\equiv \Delta p_s / \{\tfrac{1}{2}\kappa p_{-\infty} M^2_{-\infty}\} \\ &= 4\pi \sum_{n=0}^{\infty} F_n(x;0)\, Y_n(y;0) / \{\kappa p_{-\infty} M^2_{-\infty}(y)\}. \end{aligned} \tag{18}$$

The local lift $l(y)$ and the local lift coefficient $C_l(y)$ are given by

$$l(y) = \int_{-\frac{1}{2}}^{\frac{1}{2}} \Delta p_s(x,y)\,dx = 2\pi \sum_{n=0}^{\infty} \bar{F}_n^{(0)} Y_n(y;0) \tag{19}$$

and

$$C_l(y) = l(y)/\{\tfrac{1}{2}\kappa p_{-\infty} M_{-\infty}^2(y)\}$$
$$= 4\pi \sum_{n=0}^{\infty} \bar{F}_n^{(0)} Y_n(y;0)/\{\kappa p_{-\infty} M_{-\infty}^2(y)\} \tag{20}$$

respectively, where

$$\bar{F}_n^{(0)} \equiv \int_{-\frac{1}{2}}^{\frac{1}{2}} F_n(x;0)\,dx. \tag{21}$$

It is worth noting at this stage that the flow field far downstream, i.e. in the Trefftz plane, can be represented in terms of $Y_n(y;0)$, $\bar{F}_n^{(0)}$ and $\beta_n(0)$. The expressions for the far-downstream flow in the present case follow at once from those in the previous paper L, if $F_n^{(0)}$ in the latter is replaced by $\bar{F}_n^{(0)}$. For example, the increase of static pressure across the cascade Δp can be expressed as

$$\Delta p = 2\pi \bar{F}_0^{(0)} Y_0^{(0)}/\{(\mu \cos^2\gamma + \sin^2\gamma)\,t\}, \tag{22}$$

where

$$\mu \equiv 1 - \bar{M}_{-\infty}^{*2}, \tag{23}$$

$$\bar{M}_{-\infty}^{*} \equiv \left(\frac{1}{\lambda}\int_0^{\lambda} \frac{1}{M_{-\infty}^2}\,dy\right)^{-\frac{1}{2}} \tag{24}$$

and

$$Y_0^{(0)} = Y_0(y;0) = \text{constant}. \tag{25}$$

In conformity with the previous paper L, $\bar{M}_{-\infty}^{*}$ defined by (24) is hereafter referred to as the harmonic mean Mach number.

2.3. *The induced velocity*

Integrating the equation of motion, we get the z-component of the induced velocity on the (x,y)-plane in the form

$$\left[\frac{w}{U}\right]_{z=0} = -\frac{1}{\kappa p_{-\infty} M_{-\infty}^2}\left[\int_{-\infty}^{x} \frac{\partial p}{\partial z}\,dx\right]_{z=0}$$
$$= -\frac{1}{\kappa p_{-\infty} M_{-\infty}^2}\Bigg[\sum_{n=0}^{\infty} T_n \bar{F}_n^{(0)} Y_n^{(0)}(y)$$
$$+ \lim_{z\to 0}\int_{-\frac{1}{2}}^{\frac{1}{2}} d\xi \int_0^{\infty} \frac{\sin\{\alpha(x-\xi)\}}{\alpha}$$
$$\times \sum_{n=0}^{\infty} \{C_n(\alpha) + \exp(-\beta_n(\alpha)|z|)\}\,\beta_n(\alpha) F_n(\xi;\alpha)\,Y_n(y;\alpha)\,d\alpha\Bigg], \tag{26}$$

where

$$T_n = \begin{cases} \pi\mu\cos\gamma/\{t(\mu\cos^2\gamma + \sin^2\gamma)\} & \text{for } n = 0, \\ \tfrac{1}{2}\pi\beta_n^{(0)} \coth(\tfrac{1}{2}\beta_n^{(0)} t\cos\gamma) & \text{for } n = 1, 2, \ldots \end{cases} \tag{27}$$

and

$$Y_n^{(0)}(y) \equiv Y_n(y;0), \quad \beta_n^{(0)} \equiv \beta_n(0), \quad F_n^{(0)}(x) \equiv F_n(x;0). \tag{28}$$

Making $x \to +\infty$ in (26) gives the expression for the upwash in the Trefftz plane as follows:

$$\left[\frac{w_\infty}{U}\right]_{z=0} = -2\sum_{n=0}^{\infty} T_n \bar{F}_n^{(0)} Y_n^{(0)}(y)/\{\kappa p_{-\infty} M_{-\infty}^2(y)\}. \tag{29}$$

In the case of the lifting-line theory, the fact that the induced velocity at the lifting-line is just one-half of that in the Trefftz plane allows us to express the

upwash at the lifting-line in terms of $Y_n^{(0)}$, $\beta_n^{(0)}$ and $\bar{F}_n^{(0)}$. Therefore it was enough for us to solve (7) only for $\alpha = 0$. However in the case of the lifting-surface problem, we must find the solution of (7) for every real value of α over $0 < \alpha < \infty$, because it is necessary to know the induced velocity over the whole blade surface and therefore to evaluate the Fourier integral in the second term in the bracket [ ] on the right-hand side of (26). For this purpose let us rewrite (26) in a form suitable for numerical calculation.

The function $Y_n(y;\alpha)$ for any real value of α can be expanded into a series such that

$$Y_n(y;\alpha) = \sum_{m=0}^{\infty} B_{n,m}(\alpha)\, Y_m^{(0)}(y) \quad (n = 0, 1, 2, \ldots), \tag{30}$$

where the spectrum function $B_{n,m}(\alpha)$ can be determined for example by the method shown in appendix A. Then, substituting (10a) and (30) into (11) and taking into account the orthogonality of $Y_n^{(0)}$, we find that $F_n(x;\alpha)$ can be expanded in a series with the same coefficients as in (30), i.e.

$$F_n(x;\alpha) = \sum_{m=0}^{\infty} B_{n,m}(\alpha)\, F_n^{(0)}(x) \quad (n = 0, 1, 2, \ldots). \tag{31}$$

Then after some calculations as shown in appendix B, we get the expression of the upwash distribution on the blade surface in the following refined form:

$$\left[\frac{w}{U}\right]_{z=0} = -\frac{1}{\kappa p_{-\infty} M_{-\infty}^2} \int_{-\frac{1}{2}}^{\frac{1}{2}} \sum_{n=0}^{\infty} \left[T_n Y_n^{(0)} + \sum_{m=0}^{\infty} D_{n,m}(x-\xi)\, Y_m^{(0)} \right] F_n^{(0)}(\xi)\, d\xi, \tag{32}$$

where

$$D_{n,m}(x-\xi) = \frac{R_{n,m}}{x-\xi} + \int_0^{\infty} H_{n,m}(\alpha) \sin\{\alpha(x-\xi)\}\, d\alpha, \tag{33}$$

$$R_{n,m} = \lim_{\alpha \to \infty} \sum_{k=0}^{\infty} \beta_k(\alpha)\, B_{k,n}(\alpha)\, B_{k,m}(\alpha)/\alpha, \tag{34}$$

$$H_{n,m}(\alpha) = \sum_{k=0}^{\infty} \beta_k(\alpha)\{C_k(\alpha)+1\} B_{k,n}(\alpha)\, B_{k,m}(\alpha)/\alpha - R_{n,m}. \tag{35}$$

2.4. *Derivation of integral equation*

The combination of (32) with the boundary condition (5) yields the following integral equation for $F_n^{(0)}(x)$:

$$-\frac{1}{\kappa p_{-\infty} M_{-\infty}^2} \int_{-\frac{1}{2}}^{\frac{1}{2}} \sum_{n=0}^{\infty} \left[T_n Y_n^{(0)} + \sum_{m=0}^{\infty} D_{n,m}(x-\xi)\, Y_m^{(0)} \right] F_m^{(0)}(\xi)\, d\xi = f(x). \tag{36}$$

If we multiply (36) by $Y_m^{(0)}(y)$ $(m = 0, 1, 2, \ldots)$ and integrate it with respect to y over the range $(0, \lambda)$, using the orthogonality of $Y_m^{(0)}(y)$, then (36) reduces to a set of integral equations as follows:

$$\frac{1}{\kappa p_{-\infty}} \int_{-\frac{1}{2}}^{\frac{1}{2}} \sum_{n=0}^{\infty} [T_n \delta_{n,m} + D_{n,m}(x-\xi)]\, F_n^{(0)}(\xi)\, d\xi = -f(x)\, \bar{Y}_m^{(0)} \quad (m = 0, 1, 2, \ldots), \tag{37}$$

where

$$\delta_{n,m} = \begin{cases} 1 & \text{for} \quad n = m, \\ 0 & \text{for} \quad n \neq m, \end{cases} \tag{38}$$

$$\bar{Y}_m^{(0)} = \frac{1}{\lambda} \int_0^{\lambda} Y_m^{(0)}(y)\, dy. \tag{39}$$

2.5. *Reduction to linear equations*

As seen in (10a), the pressure distribution $\Delta p_s(x, y)$ is expressed as an infinite series. In numerical work, however, we are obliged to conduct calculations by omitting the coefficients $F_n^{(0)}(x)$ of order greater than some specific n. If we neglect the higher-order terms than $n = N$, then we get a set of a finite number of integral equations for $F_n^{(0)}(x)$ ($n = 0, 1, 2, \ldots, N-1$).

The chordwise variation of $\Delta p_s(x, y)$ depends upon the $F_n^{(0)}(x)$, which have to be determined from (37). The straightforward inversion of the integral equations without any approximation seems in general impossible. Therefore in order to solve (37) we have to rely upon some method of getting approximate solutions. The method preferred in this case is the well-known Glauert trigonometric series substitution, which has been applied with success to the problems of a cascade in uniform flow, for example by Scholz (1950). Thus, introducing angle variables θ, ϕ defined by

$$x = \tfrac{1}{2}\cos\theta, \quad \xi = \tfrac{1}{2}\cos\phi \quad (0 \leqslant \theta, \phi \leqslant \pi), \tag{40}$$

we expand each of $F_n^{(0)}(x)$ into the following trigonometric series:

$$\begin{aligned} F_n^{(0)}(x) = \kappa p_{-\infty}\,[&\alpha_g\,(A_{n,0}\tan\tfrac{1}{2}\theta + A_{n,1}\sin\theta + A_{n,2}\sin 2\theta + \ldots) \\ &+ \epsilon\,(E_{n,0}\tan\tfrac{1}{2}\theta + E_{n,1}\sin\theta + E_{n,2}\sin 2\theta + \ldots)], \end{aligned} \tag{41}$$

where α_g and ϵ are, as pictured in figure 1, the angle of attack and the maximum camber respectively. Therefore the slope of the blade mean camber surface $f(x)$ can be represented as

$$-f(x) = \alpha_g + \epsilon b(x). \tag{42}$$

The trigonometric series (41) is assured to contain the appropriate singularity at the leading edge as well as to satisfy the Kutta–Joukowsky condition at the trailing edge. The experimental results (Namba & Asanuma 1965) suggest to us that a series expansion like (41) is suitable also for a cascade in shear flow as long as the flow is subsonic everywhere. Another reason why this method is advantageous is that the definite integral with respect to ϕ can be evaluated in closed analytical form and that from a practical standpoint the pressure distribution is evaluated with satisfactory accuracy only from the first few terms in the series (41) as long as it is concerned with conventional thin blades.

Substituting (41) into (37), integrating with respect to ϕ over $(0, \pi)$ and separating it into the components of the angle of attack and the camber, we get the following two sets of linear algebraic equations for $A_{n,k}$ and $E_{n,k}$ ($n, k = 0, 1, 2, \ldots$) respectively:

$$\sum_{n=0}^{\infty}\sum_{k=0}^{\infty} A_{n,k}\,G_{m,n,k}(\theta) = \overline{Y}_m^{(0)}, \tag{43}$$

$$\sum_{n=0}^{\infty}\sum_{k=0}^{\infty} E_{n,k}\,G_{m,n,k}(\theta) = \overline{Y}_m^{(0)}\,b(\tfrac{1}{2}\cos\theta) \quad (m = 0, 1, 2, \ldots). \tag{44}$$

Analytical expressions of $G_{m,n,k}(\theta)$ are given in appendix C.

As mentioned above, it is permissible from a practical point of view to cut the trigonometric series (41) down to one with a finite number of terms. Then we can compute approximate values of the remaining coefficients by satisfying (43) and

(44), or in other words the boundary condition (5), at the same number of discrete points along the blade chord as the retained terms. In order to get as good an approximation as possible, it seems advantageous to apply the method used, for example, by Scholz (1950) or Schlichting (1955), which is to choose the representative points at the three-quarters station of each chord section formed by dividing the blade chord equally into as many sections as there are terms retained in the series. That is, if we are to satisfy (43) and (44) at M points along the chord, then the co-ordinates of these points are given by

$$x_n = \tfrac{1}{2}\cos\theta_n = (1/M)\,(n+\tfrac{3}{4}) - \tfrac{1}{2} \quad (n = 0, 1, 2, \ldots, M-1). \tag{45}$$

Then, if we retain N terms in the series (10a) and M terms in the series (41), we get two sets of simultaneous $N \times M$ linear equations for unknowns $A_{n,k}$ and $E_{n,k}$ ($n = 0, 1, 2, \ldots, N-1$; $k = 0, 1, 2, \ldots, M-1$) respectively, i.e.

$$\sum_{n=0}^{N-1}\sum_{k=0}^{M-1} A_{n,k}\, G_{m,n,k}(\theta_i) = \overline{Y}_m^{(0)}, \tag{46}$$

$$\sum_{n=0}^{N-1}\sum_{k=0}^{M-1} E_{n,k}\, G_{m,n,k}(\theta_i) = \overline{Y}_m^{(0)}\, b(\tfrac{1}{2}\cos\theta_i) \tag{47}$$

$$(m = 0, 1, 2, \ldots, N-1;\ i = 0, 1, 2, \ldots, M-1).$$

Once the coefficients $A_{n,k}$ and $E_{n,k}$ are determined numerically, then the pressure jump coefficient C_p can be calculated by

$$C_p = \frac{4\pi}{M_{-\infty}^2}\sum_{n=0}^{N-1}\left[\alpha_g\left(A_{n,0}\tan\tfrac{1}{2}\theta + \sum_{k=1}^{M-1} A_{n,k}\sin k\theta\right) + \epsilon\left(E_{n,0}\tan\tfrac{1}{2}\theta + \sum_{k=1}^{M-1} E_{n,k}\sin k\theta\right)\right] \tag{48}$$

and $\overline{F}_n^{(0)}$ can be obtained from (21) and (41) as

$$\overline{F}_n^{(0)} = \tfrac{1}{4}\pi[\alpha_g(A_{n,0} + \tfrac{1}{2}A_{n,1}) + \epsilon(E_{n,0} + \tfrac{1}{2}E_{n,1})]. \tag{49}$$

2.6. *Application to uniform flow and incompressible shear flow*

The present theory can be regarded as a generalized subsonic cascade theory including as special cases a cascade in subsonic uniform flow and one in incompressible shear flow. Therefore its application to these cases already studied will be instructive and useful for justification of this theory.

Subsonic uniform flow. A simple example of the procedure presented in this paper is provided by considering the solution for $M_{-\infty}(y) = M_0 =$ constant over $0 \leqslant y \leqslant \lambda$. In this case the solution of (7) for $\alpha = 0$ under the boundary condition (8) becomes

$$Y_0^{(0)} = M_0, \quad Y_n^{(0)} = \sqrt{2}\, M_0 \cos(n\pi y/\lambda) \quad (n = 1, 2, \ldots), \tag{50}$$

$$\beta_n^{(0)} = n\pi \quad (n = 0, 1, 2, \ldots). \tag{51}$$

Therefore we have

$$\overline{Y}_{n,m} = \frac{1}{\lambda}\int_0^{\lambda} Y_n^{(0)}\, Y_m^{(0)}\, dy = M_0^2\,\delta_{n,m} \tag{52}$$

and hence the matrix (A 5) reduces to a diagonal matrix from which we get

$$\beta_n(\alpha) = \sqrt{(n^2\pi^2 + \mu\alpha^2)} \quad (\mu = 1 - M_0^2), \tag{53}$$

$$B_{n\,m}(\alpha) = \delta_{n,m}. \tag{54}$$

Then equations (34) and (35) degenerate to

$$R_{n,m} = \delta_{n,m}\sqrt{\mu}, \tag{55}$$

$$H_{n,m}(\alpha) = \delta_{n,m}[\sqrt{(\mu + n^2\pi^2/\alpha^2)}\{C_n(\alpha)+1\} - \sqrt{\mu}] \tag{56}$$

respectively, and it follows from (C 1) that

$$G_{m,n,k}(\theta) = 0 \quad \text{for} \quad n \neq m. \tag{57}$$

Finally, considering (57) together with

$$\overline{Y}_n^{(0)} = \frac{1}{\lambda}\int_0^{\lambda} Y_n^{(0)}\, dy = M_0\,\delta_{0\,n}, \tag{58}$$

which follows from (50), we find that (46) and (47) reduce to the following systems of M linear equations for $A_{0,k}$ and $E_{0,k}$ $(k = 0, 1, 2, \ldots, M-1)$ respectively:

$$\sum_{k=0}^{M-1} A_{0\,k} G_{0,0,k}(\theta_i) = M_0, \tag{59}$$

$$\sum_{k=0}^{M-1} E_{0,k} G_{0,0,k}(\theta_i) = M_0 b(\tfrac{1}{2}\cos\theta_i) \quad (i = 0, 1, 2, \ldots, M-1). \tag{60}$$

Especially in the case of an isolated blade ($t = \infty$), we get from (16) and (27)

$$T_0 = 0, \quad C_0(\alpha) = 0 \tag{61}$$

and hence from (55), (56) and (C 2)

$$G_{0,0,0}(\theta) = \pi\sqrt{\mu}, \quad G_{0,0,1}(\theta) = \pi\sqrt{\mu}\cos\theta, \quad G_{0,0,2}(\theta) = \pi\sqrt{\mu}\cos 2\theta. \tag{62}$$

Consequently, if a parabolic arc blade with $b(\frac{1}{2}\cos\theta) = 4\cos\theta$ is considered, the solutions of (59) and (60) are obtained straightforwardly as

$$\begin{aligned} &A_{0,0} = \pi M_0/\sqrt{\mu}, \quad A_{0,n} = 0 \quad \text{for} \quad n = 1, 2, \ldots, \\ &E_{0,0} = 0, \quad E_{0,1} = 4\pi M_0/\sqrt{\mu}, \quad E_{0,n} = 0 \quad \text{for} \quad n = 2, 3, \ldots, \end{aligned} \tag{63}$$

and therefore from (48), (49) and (20) we get

$$C_p = 4(\alpha_y \tan\tfrac{1}{2}\theta + 4\epsilon\sin\theta)/\sqrt{\mu}, \tag{64}$$

$$C_l = 2\pi(\alpha_g + 2\epsilon)/\sqrt{\mu}, \tag{65}$$

which completely agree with the two-dimensional thin aerofoil theory based on the Prandtl–Glauert rule.

Incompressible shear flow. The solution for an incompressible shear flow with prescribed velocity distribution of $U(y)$ can be obtained by replacing $M_{-\infty}^2$ by $U^2(y)/c_{-\infty}^2$, where $c_{-\infty}^2 = \kappa p_{-\infty}/\rho_{-\infty}$ and taking the limit $c_{-\infty}^2 \to \infty$ with $U(y)$ fixed. If we put

$$Y_n^{(0)\prime} = c_{-\infty} Y_n^{(0)}, \quad A'_{n,k} = c_{-\infty} A_{n,k}, \quad E'_{n,k} = c_{-\infty} E_{n,k}, \tag{66}$$

then (9), (43) and (44) indicate that $Y_n^{(0)\prime}$, $A'_{n,k}$ and $E'_{n,k}$ are independent of $c_{-\infty}$. Considering that $\overline{Y}_n^{(0)} = O(c_{-\infty}^{-1})$ as $c_{-\infty} \to \infty$, we find that as $c_{-\infty} \to \infty$ the matrix (A 5) again reduces to a diagonal matrix and hence we get

$$\left.\begin{aligned} \beta_n(\alpha) &= \sqrt{(\beta_n^{(0)2} + \alpha^2)}, \\ B_{n,m}(\alpha) &= \delta_{m,n}, \\ R_{n,m} &= \delta_{m,n}, \\ H_{n,m}(\alpha) &= \delta_{m\,n}[\sqrt{(1 + \beta_n^{(0)2}/\alpha^2)}\{C_n(\alpha)+1\} - 1]. \end{aligned}\right\} \tag{67}$$

From the above relations it follows that

$$G_{m,n,k}(\theta) = 0 \quad \text{for} \quad n \neq m. \tag{68}$$

Hence a set of $N \times M$ linear equations (46) or (47) degenerates to N sets of M linear equations as follows:

$$\sum_{k=0}^{M-1} A'_{n,k} G_{n,n,k}(\theta_i) = \overline{Y}_n^{(0)\prime}, \tag{69}$$

$$\sum_{k=0}^{M-1} E'_{n,k} G_{n,n,k}(\theta_i) = \overline{Y}_n^{(0)\prime} b\left(\tfrac{1}{2}\cos\theta_i\right)$$
$$(n = 0, 1, 2, \ldots, N-1;\ i = 0, 1, 2, \ldots, M-1). \tag{70}$$

Comparison of (69) and (70) with (46) and (47) indicates that contrary to the case of compressible shear flow the nth components $A'_{n,k}$ and $E'_{n,k}$ in this case become independent of those of order other than n.

3. Numerical examples

3.1. *Specification of flow model and remarks on numerical computation*

The Mach number profile adopted is of the same type as that in L, i.e.

$$M_{-\infty}(y) = M_0 \exp(ay/\lambda). \tag{71}$$

Therefore $Y_n^{(0)}$ and $\beta_n^{(0)}$ are given by

$$Y_0^{(0)} = \overline{M}^*_{-\infty} = M_0\{2a\, e^{2a}/(e^{2a}-1)\}^{\frac{1}{2}},$$

$$Y_n^{(0)} = \sqrt{2}\, M_0 a (a^2 + n^2\pi^2)^{-\frac{1}{2}} e^{2ay/\lambda}\left(\sin\frac{n\pi y}{\lambda} - \frac{n\pi}{a}\cos\frac{n\pi}{\lambda}\right),$$

$$\beta_0^{(0)} = 0,$$

$$\beta_n^{(0)} = (a^2 + n^2\pi^2)^{\frac{1}{2}}/\lambda \quad (n = 1, 2, \ldots).$$

In this paper numerical examples are shown for three different Mach number levels with the shear parameter $a \equiv \lambda(dM_{-\infty}/dy)/M_{-\infty}$ held constant at a value of 1·0, namely (i) $M_0 = M_1 = 0$, (ii) $M_0 = 0{\cdot}270$, $M_1 = 0{\cdot}734$, (iii) $M_0 = 0{\cdot}367$, $M_1 = 0{\cdot}998$. Here $M_1 = M_{-\infty}(\lambda) = M_0 e^a$ and the case (i) means an incompressible shear flow.

The blade profiles adopted are a flat plate and a parabolic arc profile, i.e. $b(x) = 4\cos\theta$.

In the numerical work solving (46) and (47) we set $N = 10$ and $M = 3$, which are considered to give a satisfactory approximation from a practical standpoint. Solving a set of linear equations (46) or (47) for 30 unknowns is not hard work for a modern high-speed electronic computer. Rather, a greater part of the time is spent in computation of the Fourier integrals in $G_{m,n,k}(\theta_i)$ given by (C 2). Since the integrands contain the trigonometric and the Bessel functions, the numerical integration requires a large number of representative abscissae of α, for each of which $\beta_n(\alpha)$ and $B_{n,m}(\alpha)$ must be computed as eigenvalues and eigenvectors of a 10×10 matrix.

In general the $H_{n,m}(\alpha)$ in the integrands are found to have a finite number of zero points for $0 < \alpha < \infty$ and they are of the order of α^{-2} for large α. Besides, since

$$J_n\left(\frac{\alpha}{2}\right) \sim \sqrt{\left(\frac{1}{\pi\alpha}\right)} \cos\left(\frac{\alpha}{2} - \frac{2n+1}{4}\pi\right) \quad \text{as} \quad \alpha \to \infty,$$

the integrands are of the order of $\alpha^{-2.5}$ for large α.

The method of numerical integration adopted is to approximate an infinite integral by a finite series summation such that

$$\int_0^\infty h(\alpha)\, d\alpha \approx \sum_{n=0}^{K} I_n,$$

where

$$I_n = \alpha_T \sum_{i=1}^{6} h\{\alpha_T(n+\zeta_i)\} w_i,$$

and ζ_i and w_i are respectively the argument values and the weights for the six point Gaussian quadrature formula. The integration interval α_T is adopted as $\alpha_T = 4\pi/(1+\cos\theta_2)$. The number of zero points of the integrands to be contained in the interval α_T is at most two in this case where $M = 3$. The summation is conducted until the last term I_K becomes so small that $|I_K| \Big/ \left|\sum_{n=0}^{K} I_n\right| < 10^{-3}$.

It is confirmed that application of this method to a cascade of flat plates in a uniform subsonic flow gives an error less than 0·5 % in comparison with the method of conformal mapping. The computation was conducted on the electronic computer HITAC 5020E at the Computing Center of the University of Tokyo. The time consumed in computation was about 200 seconds for each case.

3.2. *Remarks on the lifting-line theory*

As mentioned previously, the purpose of this paper is to make clear the compressibility effect by a complete three-dimensional theory, that is, the lifting-surface theory. For this purpose it will be instructive to make a comparison between the lifting-surface theory and the lifting-line theory given in L. The latter is considered to be incomplete as a three-dimensional theory as far as the compressibility effect is concerned. The most convenient factor for elucidating the difference between the theories is the derivative of the local lift coefficient with respect to the local effective angle of attack defined by

$$K = (\partial C_l/\partial\alpha_0)_{\alpha_0=0} = C_l(y)/\alpha_0, \tag{72}$$

where α_0 is the effective angle of attack defined as

$$\alpha_0 = \alpha_{-\infty} + \tfrac{1}{2}[w_\infty/U]_{z=0} \tag{73}$$

and $\alpha_{-\infty}$ is the angle of attack measured from the zero-lift angle. The lifting-line theory consists essentially in assuming $K(y)$ to be equal to the value in the two-dimensional flow of the Mach number corresponding to $M_{-\infty}(y)$, that is, K in the lifting-line theory is given by

$$K = K^{(2D)}(M_{-\infty}(y)), \tag{74}$$

where the superscript $(2D)$ denotes the two-dimensional flow condition. Here $K^{(2D)}$ is calculated by using the two-dimensional linearized cascade theory including the Prandtl–Glauert rule.

3.3. *Discussion on the numerical results*

Figures 2, 3 and 4 show examples of the spanwise distributions of the local lift coefficient C_l, the upwash in the Trefftz plane $[w_\infty/U]_{z=0}$ and K defined by (72) respectively, where $C_{L,i}^{(2D)}$ used for normalization denotes the lift coefficient in

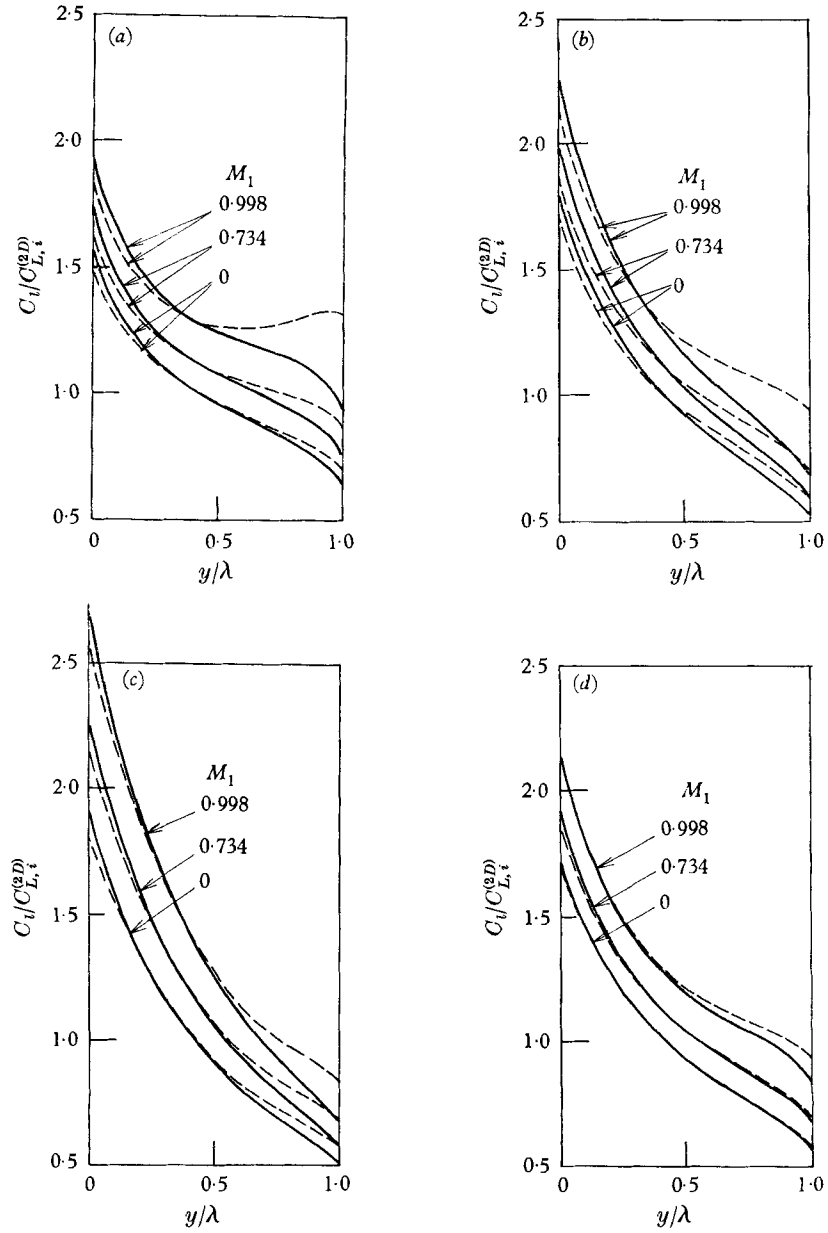

FIGURE 2. Spanwise distribution of the local lift coefficient in shear flows of $a = 1{\cdot}0$. ———, lifting-surface theory; – – –, lifting-line theory. (*a*) An isolated flat plate of $\lambda = 5{\cdot}0$. (*b*) An isolated flat plate of $\lambda = 2{\cdot}5$. (*c*) A cascade of flat plates of $t = 1{\cdot}0$, $\gamma = 60°$ and $\lambda = 2{\cdot}5$. (*d*) An isolated parabolic arc blade of $\lambda = 2{\cdot}5$.

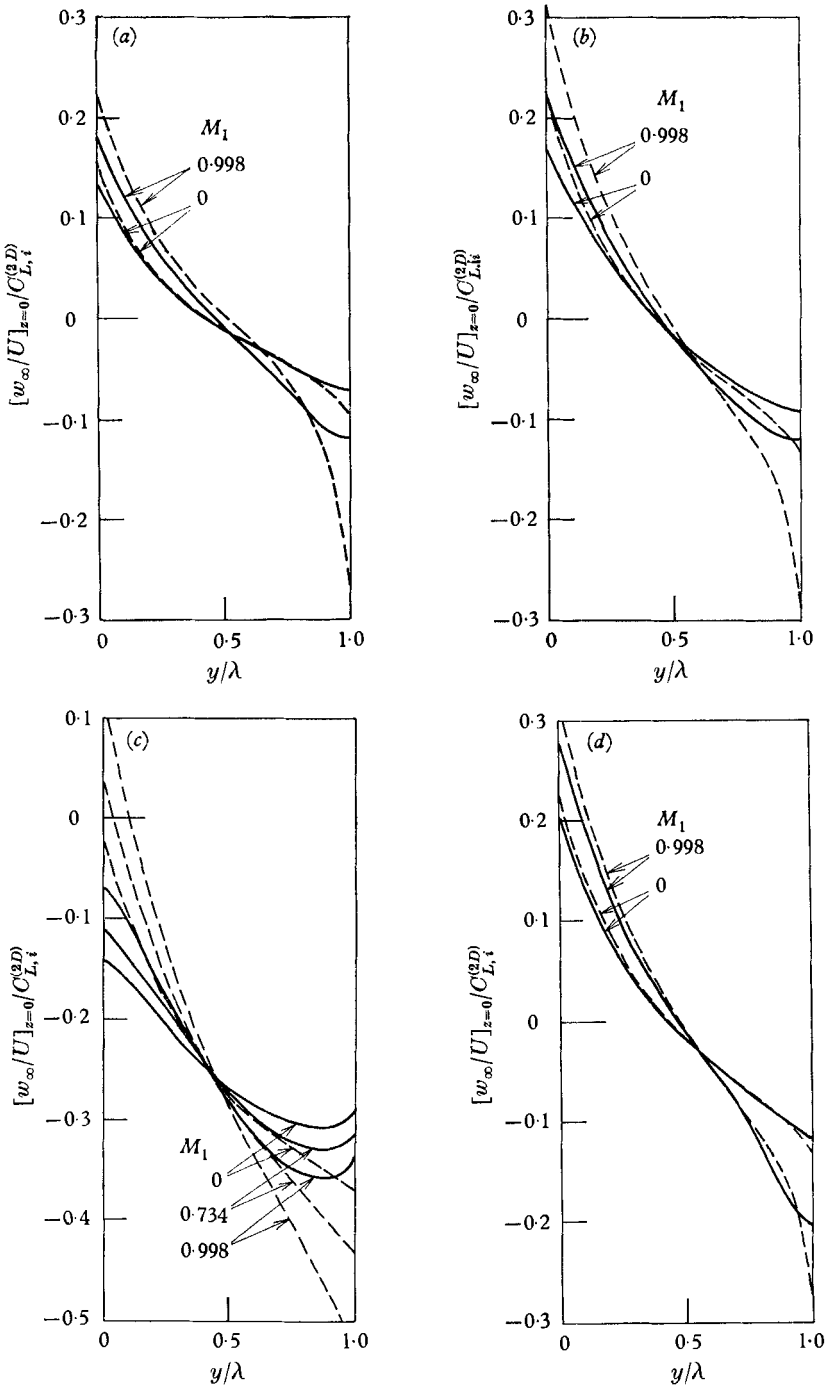

FIGURE 3. Spanwise distribution of the z-component of the induced velocity on the wake surface far downstream in shear flows of $a = 1{\cdot}0$. ———, lifting-surface theory; – – –, lifting-line theory. (*a*) An isolated flat plate of $\lambda = 5{\cdot}0$. (*b*) An isolated flat plate of $\lambda = 2{\cdot}5$. (*c*) A cascade of flat plates of $t = 1{\cdot}0$, $\gamma = 60°$ and $\lambda = 2{\cdot}5$. (*d*) An isolated parabolic arc blade of $\lambda = 2{\cdot}5$.

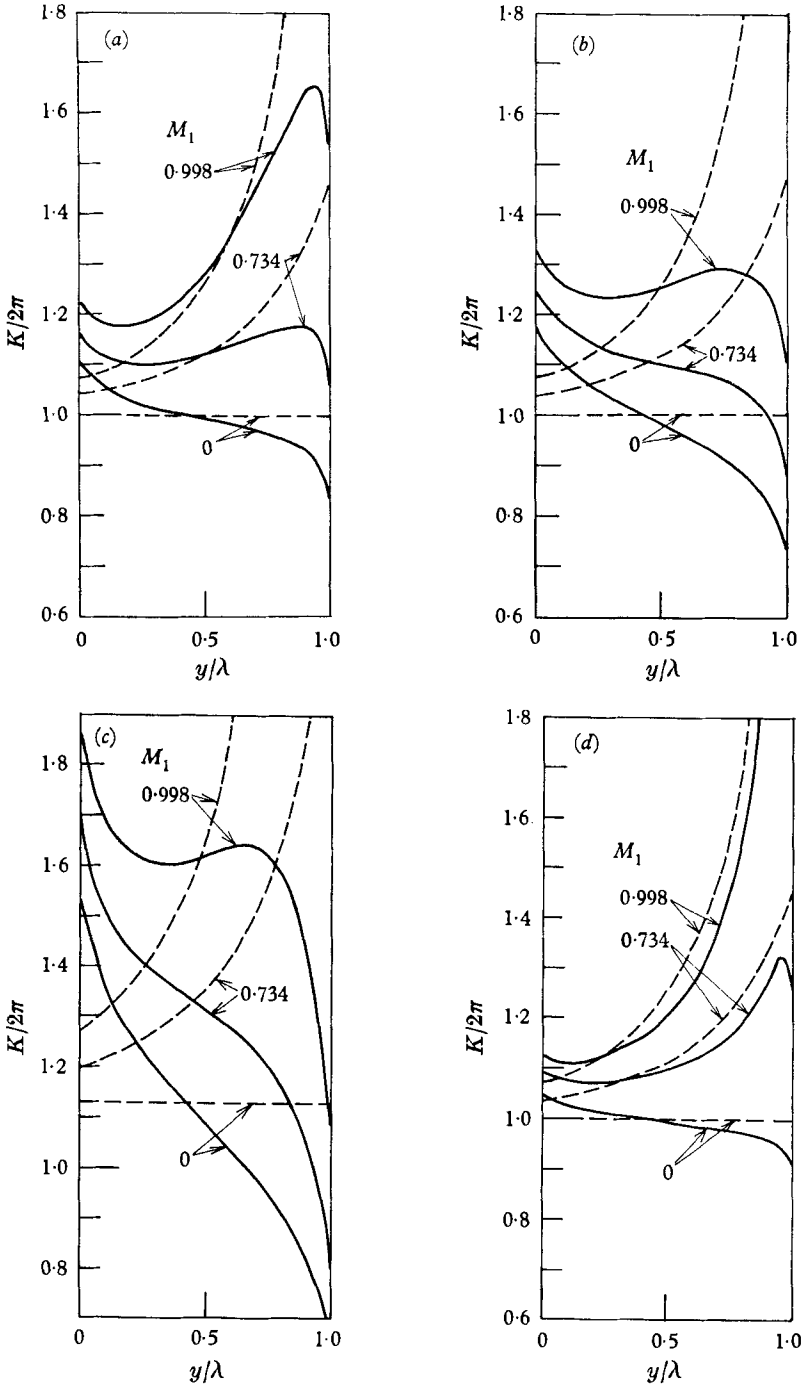

FIGURE 4. Spanwise distribution of the derivative of the local lift coefficient with respect to the local effective angle of attack in shear flows of $a = 1{\cdot}0$. ———, lifting-surface theory; – – –, lifting-line theory. (*a*) An isolated flat plate of $\lambda = 5{\cdot}0$. (*b*) An isolated flat plate of $\lambda = 2{\cdot}5$. (*c*) A cascade of flat plates of $t = 1{\cdot}0$, $\gamma = 60°$ and $\lambda = 2{\cdot}5$. (*d*) An isolated parabolic arc blade of $\lambda = 2{\cdot}5$.

two-dimensional incompressible flow. Also presented for comparison with the dotted lines are the corresponding distributions according to the lifting-line theory. Examples of the chordwise distributions of pressure at three different span-stations are demonstrated in figures 5, 6 and 7 for three different cascade conditions. The dotted lines in these figures are the chordwise distributions calculated according to the lifting-line theory, by which we mean those in the two-

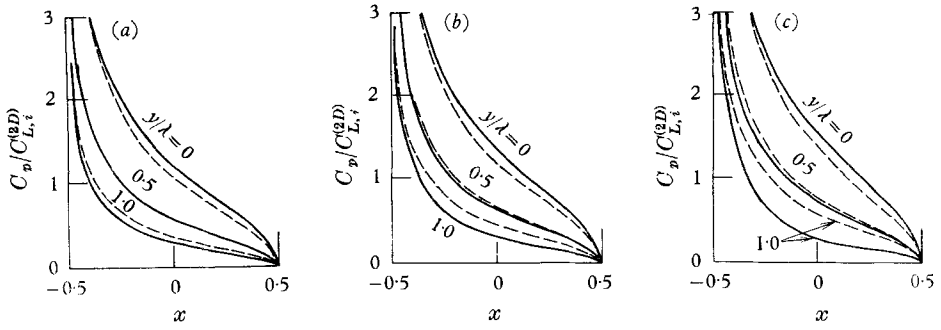

FIGURE 5. Chordwise distribution of the pressure coefficient for an isolated flat plate of $\lambda = 2{\cdot}5$ in shear flows of $a = 1{\cdot}0$. ———, lifting-surface theory; – – –, lifting-line theory. (*a*) $M_0 = M_1 = 0$ (incompressible shear flow). (*b*) $M_0 = 0{\cdot}270$, $M_1 = 0{\cdot}734$. (*c*) $M_0 = 0{\cdot}367$, $M_1 = 0{\cdot}998$.

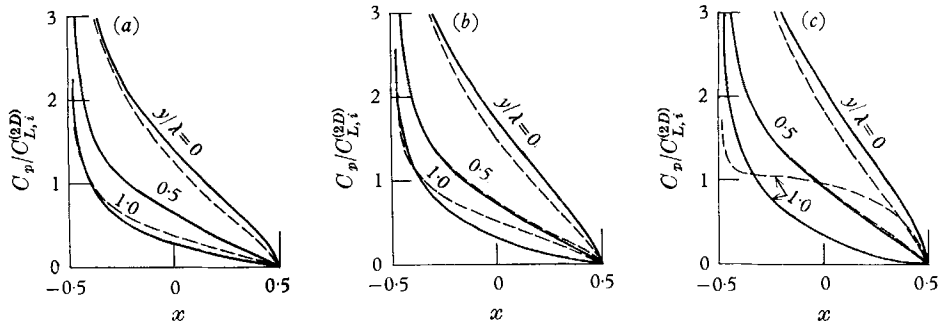

FIGURE 6. Chordwise distribution of the pressure coefficient for a cascade of flat plates of $t = 1{\cdot}0$, $\gamma = 60°$ and $\lambda = 2{\cdot}5$ in shear flows of $a = 1{\cdot}0$. ———, lifting-surface theory; – – –, lifting-line theory. (*a*) $M_0 = M_1 = 0$ (incompressible shear flow). (*b*) $M_0 = 0{\cdot}270$, $M_1 = 0{\cdot}734$. (*c*) $M_0 = 0{\cdot}367$, $M_1 = 0{\cdot}998$.

dimensional flows at the Mach number corresponding to the local ones in the undisturbed shear flow as well as at the angle of attack corresponding to the local effective angle of attack based upon the lifting-line theory.

As seen from figure 4 the validity of the assumption in the lifting-line theory, i.e. quasi-two-dimensionality in the effect of compressibility, becomes poorer as the Mach number level increases and as the aspect ratio λ decreases. As far as the examples demonstrated in figure 4 are concerned, the lifting-line theory seems more valid for the cambered isolated blade than for the isolated flat plate. It would be unwise, however, to be hasty in generalization. In fact as regards the chordwise pressure distributions in figures 5, 6 and 7, the difference between the theories seems largest for the cambered blade. The reason why such a large difference in C_p distribution between both theories yields rather small influence

on the differences in the integrated values such as K or C_l is that the disturbance pressure on the cambered blade can change its sign along the chord at a lower angle of attack.

Another striking feature of the results is the relatively small difference in the local lift distribution between the theories. The reason for this will be obvious from the downwash distributions in figure 3. The larger values of K at the higher Mach number span-station according to the lifting-line theory is associated with stronger trailing vorticity which in turn brings about the stronger downwash.

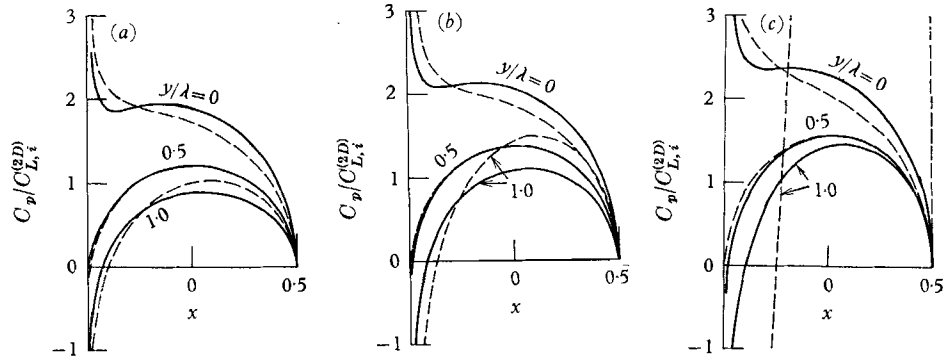

FIGURE 7. Chordwise distribution of the pressure coefficient for an isolated parabolic arc blade of $\lambda = 2{\cdot}5$ in shear flows of $a = 1{\cdot}0$. ———, lifting-surface theory; – – –, lifting-line theory. (*a*) $M_0 = M_1 = 0$ (incompressible shear flow). (*b*) $M_0 = 0{\cdot}270$, $M_1 = 0{\cdot}734$. (*c*) $M_0 = 0{\cdot}367$, $M_1 = 0{\cdot}998$.

Because the downwash makes the effective angle of attack decrease, the net balance of the lift force at the higher Mach number station due to lifting-line theory shows no extremely large difference from that according to the lifting-surface theory. Whatever the reason, one may conclude that the lifting-line theory can safely be used for the reasonable prediction of the lift distribution as long as the maximum Mach number of the shear flow is lower than about 0·8.

In general, however, the lifting-line theory gives significant error at near-sonic stations. Here it should be emphasized that the lifting-surface theory gives no such great value of K or C_l at near-sonic span-stations as would be expected from the two-dimensional Prandtl–Glauert rule. This result suggests to us that the relatively small lift force at near-sonic span-stations in shear flow gives less liability of occurrence of shock waves in shear flow than in uniform flow and that a flow pattern according to the three-dimensional linear theory can physically exist even in high subsonic or transonic shear flow. As stated earlier in this paper the author's (1965) experimental results may provide a justification of this conjecture.

4. Conclusion

A lifting-surface theory for a cascade of blades in subsonic shear flow has been developed. Numerical examples are provided and compared with the results according to lifting-line theory.

The dependence of the local lift force upon the local Mach number at near-sonic span-stations in a shear flow shows a great deviation from that according to the uniform flow theory which is applied to the lifting-line theory. In shear flows no extremely great lift force appears at near-sonic span-stations even within the scope of the linearized theory.

As far as the effect of non-uniform Mach number upon the spanwise distribution of the lift force is concerned, the evaluation according to the lifting-line theory gives no significant error in comparison with the lifting-surface theory if the maximum Mach number of the shear flow is below about 0·8.

The chordwise distribution of the surface pressure at high subsonic span-stations in a shear flow deviates significantly from that in the corresponding two-dimensional flow with the angle of attack corrected according to the lifting-line theory.

The author wishes to express his gratitude to Prof. T. Asanuma and Associate Prof. Y. Tanida of the Institute of Space and Aeronautical Science, University of Tokyo, as well as to Profs. T. Okazaki and J. Kondo of the Department of Aeronautics, University of Tokyo, for their valuable discussions and encouragement.

Appendix A. Solution of (8) and (9)

As is shown in L, the solution of the boundary-value problem (8) and (9) for $\alpha = 0$, i.e. $Y_n^{(0)}$ and $\beta_n^{(0)}$, can be obtained in analytical forms when the basic shear flow has some special Mach number profiles, for example an exponential or a linear profile. Then, assume that $Y_n^{(0)}$ and $\beta_n^{(0)}$ are known and represent Y for any real value of α in terms of an infinite series such that

$$Y = \sum_{n=0}^{\infty} \beta_n(\alpha)\, Y_n^{(0)}(y). \tag{A 1}$$

Substitution of (A 1) into (8) gives

$$\frac{1}{M_{-\infty}^2(y)} \sum_{n=0}^{\infty} [\beta^2 - \beta_n^{(0)2} - \alpha^2 \{1 - M_{-\infty}^2(y)\}]\, B_n(\alpha)\, Y_n^{(0)}(y) = 0. \tag{A 2}$$

Multiplying (A 2) by $Y_m^{(0)}$, integrating with respect to y from 0 to λ and taking into account the orthogonality of $Y_m^{(0)}$, we get simultaneous homogeneous linear equations for $B_m(\alpha)$ $(m = 0, 1, 2, \ldots)$ as follows:

$$B_m(\alpha)(\beta_m^{(0)2} - \alpha^2 - \beta^2) + \alpha^2 \sum_{n=0}^{\infty} B_n(\alpha)\, \overline{Y}_{n,m} = 0 \quad (m = 0, 1, 2, \ldots), \tag{A 3}$$

where

$$\overline{Y}_{n,m} \equiv \frac{1}{\lambda} \int_0^{\lambda} Y_n^{(0)} Y_m^{(0)}\, dy. \tag{A 4}$$

Therefore β_n^2/α^2 $(n = 0, 1, 2, \ldots)$ are obtainable as the eigenvalues of a symmetric infinite matrix given by

$$\Delta \equiv \begin{Bmatrix} 1 - \overline{Y}_{0,0} + \beta_0^{(0)2}/\alpha^2 & -\overline{Y}_{0,1} & -\overline{Y}_{0,2} & \cdots \\ -\overline{Y}_{1,0} & 1 - \overline{Y}_{1,1} + \beta_1^{(0)2}/\alpha^2 & -\overline{Y}_{1,2} & \cdots \\ -\overline{Y}_{2,0} & -\overline{Y}_{2,1} & 1 - \overline{Y}_{2,2} + \beta_2^{(0)2}/\alpha^2 & \cdots \\ \cdots & \cdots & \cdots & \cdots \end{Bmatrix} \tag{A 5}$$

and $[B_{n,0}(\alpha), B_{n,1}(\alpha), B_{n,2}(\alpha), \ldots]$ $(n = 0, 1, 2, \ldots)$ are the corresponding eigenvectors. Using $B_{n,m}(\alpha)$, we can get the eigenfunction $Y_n(y;\alpha)$ for any real value of α as

$$Y_n(y;\alpha) = \sum_{m=0}^{\infty} B_{n,m}(\alpha)\, Y_m^{(0)}(y). \tag{A 6}$$

In order to determine $B_{n,m}(\alpha)$ and $\beta_n(\alpha)$ numerically, it is necessary, in general, to use a finite matrix as an approximation to (A 5).

Appendix B. Derivation of (32)

Denoting the second term in the square bracket [ ] on the right-hand side of (26) by I, and dividing the infinite integral in I into three parts, we get

$$\begin{aligned} I = \lim_{z\to 0} \int_{-\frac{1}{2}}^{\frac{1}{2}} d\xi \int_0^{\infty} \frac{\sin\{\alpha(x-\xi)\}}{\alpha} \sum_{n=0}^{\infty} \exp(-\beta_n(\alpha)|z|) C_n(\alpha)\beta_n(\alpha) F_n(\xi;\alpha) Y_n(y;\alpha)\, d\alpha \\ + \lim_{z\to 0} \int_{-\frac{1}{2}}^{\frac{1}{2}} d\xi \int_0^{\infty} \sin\{\alpha(x-\xi)\} \sum_{n=0}^{\infty} \exp(-\beta_n(\alpha)|z|) \\ \times \left[\frac{\beta_n(\alpha)}{\alpha} F_n(\xi;\alpha) Y_n(y;\alpha) - \lim_{\alpha\to\infty} \frac{\beta_n(\alpha)}{\alpha} F_n(\xi;\alpha) Y_n(y;\alpha)\right] d\alpha \\ + \lim_{z\to 0} \int_{-\frac{1}{2}}^{\frac{1}{2}} d\xi \sum_{n=0}^{\infty} \lim_{\alpha\to\infty} \left\{\frac{\beta_n(\alpha)}{\alpha} F_n(\xi;\alpha) Y_n(y;\alpha)\right\} \\ \times \int_0^{\infty} \sin\{\alpha(x-\xi)\} \exp(-\beta_n(\alpha)|z|)\, d\alpha. \end{aligned} \tag{B 1}$$

Examination of the matrix (A 5) reveals that

$$\left.\begin{aligned} \beta_n(\alpha)/\alpha &\sim q_n + O(\alpha^{-2}) \\ B_{n,m}(\alpha) &\sim B_{n,m}(\infty) + O(\alpha^{-2}) \end{aligned}\right\} \quad \text{as} \quad \alpha\to\infty$$

and hence from (30) and (31)

$$\left.\begin{aligned} Y_n(y;\alpha) &\sim Y_n(y;\infty) + O(\alpha^{-2}) \\ F_n(x;\alpha) &\sim F_n(x;\infty) + O(\alpha^{-2}) \end{aligned}\right\} \quad \text{as} \quad \alpha\to\infty,$$

where q_n, $B_{n,m}(\infty)$, $Y_n(y;\infty)$ and $F_n(x;\infty)$ are finite values. Furthermore from (16)

$$C_n(\alpha) \sim -2\exp(-2\beta_n(\alpha)\, t\cos\gamma) \sim -2\exp(-2q_n\alpha t\cos\gamma)$$

as $\alpha\to\infty$. From this limiting behaviour, it is found that the Fourier integrals in the first and second terms on the right-hand side of (B 1) converge uniformly with respect to z. As to the Fourier integral in the third term, we can apply Abel's summation theorem to it as follows:

$$\begin{aligned} \lim_{z\to 0} \int_0^{\infty} \sin\{\alpha(x-\xi)\} \exp(-\beta_n(\alpha)|z|)\, d\alpha \\ = \lim_{z\to 0} \int_0^{\infty} \sin\{\alpha(x-\xi)\} \exp(-q_n\alpha|z|)\, d\alpha = \frac{1}{x-\xi}. \end{aligned}$$

Consequently (B 1) becomes

$$\begin{aligned} I = \int_{-\frac{1}{2}}^{\frac{1}{2}} d\xi \int_0^{\infty} \sin\{\alpha(x-\xi)\} \sum_{n=0}^{\infty} \left[\frac{\beta_n(\alpha)}{\alpha}\{C_n(\alpha)+1\} F_n(\xi;\alpha) Y_n(y;\alpha)\right. \\ \left. - q_n F_n(\xi;\infty) Y_n(y;\infty)\right] d\alpha + \int_{-\frac{1}{2}}^{\frac{1}{2}} \frac{1}{x-\xi} \sum_{n=0}^{\infty} q_n F_n(\xi;\infty) Y_n(y;\infty)\, d\xi. \end{aligned} \tag{B 2}$$

Then, substitution of (30) and (31) into (B 2) gives after some arrangement

$$I = \int_{-\frac{1}{2}}^{\frac{1}{2}} \sum_{m=0}^{\infty} F_m^{(0)}(\xi) \sum_{k=0}^{\infty} Y_k^{(0)}(y) \left[\int_0^{\infty} \sin\{\alpha(x-\xi)\} H_{m,k}(\alpha)\, d\alpha + \frac{R_{m,k}}{x-\xi} \right] d\xi,$$

where $H_{m,k}(\alpha)$ and $R_{m,k}$ are defined by (34) and (35) respectively. Using the above expression, we finally get the expression (32).

Appendix C. Expressions of $G_{m,n,k}(\theta)$

Equations (43) and (44) are obtained by defining $G_{m,n,k}(\theta)$ as

$$\left.\begin{aligned} G_{m,n,0}(\theta) &= \frac{1}{2}\int_0^{\pi} [T_n \delta_{n,m} + D_{n,m}(\tfrac{1}{2}\cos\theta - \tfrac{1}{2}\cos\phi)] \tan\tfrac{1}{2}\phi \sin\phi\, d\phi, \\ G_{m,n,k}(\theta) &= \frac{1}{2}\int_0^{\pi} [T_n \delta_{n,m} + D_{n,m}(\tfrac{1}{2}\cos\theta - \tfrac{1}{2}\cos\phi)] \sin k\phi \sin\phi\, d\phi, \end{aligned}\right\} \quad (k = 1, 2, \ldots). \tag{C 1}$$

The expression of $D_{n,m}(x-\xi)$ given by (33) indicates that conduction of integration with respect to ϕ in (C 1) needs evaluation of some definite integrals as follows:

First,

$$\int_0^{\pi} \tan\tfrac{1}{2}\phi \sin\phi\, d\phi = \pi,$$

$$\int_0^{\pi} \sin k\phi \sin\phi\, d\phi = \begin{cases} \frac{1}{2}\pi & \text{for } k = 1, \\ 0 & \text{for } k = 2, 3, \ldots. \end{cases}$$

Secondly,

$$\int_0^{\pi} \frac{\tan\frac{1}{2}\phi}{\cos\theta - \cos\phi} \sin\phi\, d\phi = \pi,$$

$$\int_0^{\pi} \frac{\sin k\phi}{\cos\theta - \cos\phi} \sin\phi\, d\phi = \pi \cos k\theta,$$

where the well-known formula

$$\int_0^{\pi} \frac{\cos k\phi}{\cos\theta - \cos\phi}\, d\phi = \frac{\pi \sin k\theta}{\sin\theta},$$

is used.

Finally, consider the formulae (Watson 1944)

$$\sin(\tfrac{1}{2}\alpha\cos\phi) = 2\sum_{n=0}^{\infty} (-1)^n \cos(2n+1)\phi\, J_{2n+1}(\tfrac{1}{2}\alpha),$$

$$\cos(\tfrac{1}{2}\alpha\cos\phi) = \sum_{n=0}^{\infty} \epsilon_n (-1)^n \cos 2n\phi\, J_{2n}(\tfrac{1}{2}\alpha),$$

where

$$\epsilon_n = \begin{cases} 1 & \text{for } n = 0, \\ 2 & \text{for } n = 1, 2, \ldots, \end{cases}$$

and J_n is the Bessel function of the first kind of order n.

Then we have

$$\int_0^\pi \tan\tfrac{1}{2}\phi \sin\{\alpha(\tfrac{1}{2}\cos\theta - \tfrac{1}{2}\cos\phi)\}\sin\phi\, d\phi$$
$$= \pi[\sin(\tfrac{1}{2}\alpha\cos\theta)\, J_0(\tfrac{1}{2}\alpha) + \cos(\tfrac{1}{2}\alpha\cos\theta)\, J_1(\tfrac{1}{2}\alpha)],$$
$$\int_0^\pi \sin\{(2n-1)\phi\}\sin\{\alpha(\tfrac{1}{2}\cos\theta - \tfrac{1}{2}\cos\phi)\}\sin\phi\, d\phi$$
$$= 2\pi\sin(\tfrac{1}{2}\alpha\cos\theta)(-1)^{n+1}\{(2n-1)/\alpha\}\, J_{2n-1}(\tfrac{1}{2}\alpha),$$
$$\int_0^\pi \sin(2n\phi)\sin\{\alpha(\tfrac{1}{2}\cos\theta - \tfrac{1}{2}\cos\phi)\}\sin\phi\, d\phi$$
$$= -2\pi\cos(\tfrac{1}{2}\alpha\cos\theta)(-1)^{n+1}(2n/\alpha)\, J_{2n}(\tfrac{1}{2}\alpha).$$

Using the relations shown above, we get the expressions of $G_{m,n,k}(\theta)$ as follows:

$$G_{m,n,0}(\theta) = \tfrac{1}{2}\pi T_n \delta_{n,m} + \pi R_{m,n}$$
$$+ \tfrac{1}{2}\pi\int_0^\infty [\sin(\tfrac{1}{2}\alpha\cos\theta)\, J_0(\tfrac{1}{2}\alpha) + \cos(\tfrac{1}{2}\alpha\cos\theta)\, J_1(\tfrac{1}{2}\alpha)]\, H_{m\,n}(\alpha)\, d\alpha,$$
$$G_{m,n,1}(\theta) = \tfrac{1}{4}\pi T_n \delta_{n,m} + \pi R_{m,n}\cos\theta$$
$$+ \pi\int_0^\infty \frac{1}{\alpha}\sin(\tfrac{1}{2}\alpha\cos\theta)\, J_1(\tfrac{1}{2}\alpha)\, H_{n,m}(\alpha)\, d\alpha,$$
$$G_{m,n,2}(\theta) = \pi R_{m,n}\cos 2\theta$$
$$- 2\pi\int_0^\infty \frac{1}{\alpha}\cos(\tfrac{1}{2}\alpha\cos\theta)\, J_2(\tfrac{1}{2}\alpha)\, H_{m,n}(\alpha)\, d\alpha. \qquad \text{(C 2)}$$

Appendix D. Expression of disturbance pressure due to a pressure dipole

Here we consider an elementary solution for a single pressure dipole of unit strength with its axis in the z-direction. The disturbance pressure p due to such a pressure dipole placed at a point $(\xi, \eta, 0)$ in a basic subsonic shear flow as shown in figure 1 must satisfy (1), except at the singular point $(\xi, \eta, 0)$, as well as the boundary conditions (4) and

$$p \to 0 \quad \text{as} \quad x^2 + z^2 \to \infty. \qquad \text{(D 1)}$$

Furthermore the singularity at $(\xi, \eta, 0)$ should be of such a character that

$$p \to \operatorname{sgn} z\, \delta(x-\xi)\,\delta(y-\eta) \quad \text{as} \quad z \to \pm 0. \qquad \text{(D 2)}$$

Applying the method of separation of variables to (1), we can get the required solution in the following Fourier integral form:

$$p = \operatorname{sgn} z \frac{1}{\pi}\int_0^\infty \cos\{\alpha(x-\xi)\}\sum_{n=0}^{\infty} \exp(-\beta_n(\alpha)|z|)\, \frac{1}{\lambda M^2_{-\infty}(\eta)}\, Y_n(\eta;\alpha)\, Y_n(y;\alpha)\, d\alpha. \qquad \text{(D 3)}$$

Since $Y_n(y;\alpha)$ and $\beta_n(\alpha)$ are respectively the eigenfunction and the eigenvalue for the Sturm–Liouville type boundary-value problem (7) and (8), it is evident that (D 3) satisfies (4). As is shown in the reference L, $\beta_n^2(\alpha)$ is positive for $0 < \alpha < \infty$, when the basic flow is subsonic everywhere, and here $\beta_n(\alpha)$ is chosen

as positive. Then considering that $Y_n(y;\alpha)$ is bounded for $0 < \alpha < \infty$ and that each of $\beta_n(\alpha)/\alpha$ tends to a finite value as $\alpha \to \infty$, we find

$$\int_0^\infty \left| \sum_{n=0}^{\infty} \exp(-\beta_n(\alpha)|z|) \frac{1}{\lambda} \frac{1}{M_{-\infty}^2(\eta)} Y_n(\eta;\alpha)\, Y_n(y;\alpha) \right| d\alpha < \infty,$$

for $z \neq 0$. Consequently it is confirmed that (D 1) is satisfied. Furthermore, since the delta function $\delta(x-\xi)$ or $\delta(y-\eta)$ can be represented formally as

$$\delta(x-\xi) = \frac{1}{\pi} \int_0^\infty \cos\{\alpha(x-\xi)\}\, d\alpha,$$

$$\delta(y-\eta) = \sum_{n=0}^{\infty} \frac{1}{\lambda} \frac{1}{M_{-\infty}^2(\eta)} Y_n(\eta;\alpha)\, Y_n(y;\alpha),$$

the condition of singularity (D 2) is also satisfied.

An expression of p due to a sheet of pressure dipoles, i.e. a lifting-surface with the dipole strength $-\frac{1}{2}\Delta p_s(x,y)$ distributed in the region $-\frac{1}{2} < x < \frac{1}{2}$, $0 < y < \lambda$, $z = 0$ can easily be derived by integrating the elementary solution (D 3) as

$$\begin{aligned} p &= -\operatorname{sgn} z \frac{1}{2\pi} \int_{-\frac{1}{2}}^{\frac{1}{2}} d\xi \int_0^\lambda \Delta p_s(\xi,\eta)\, d\eta \\ &\quad \times \int_0^\infty \cos\{\alpha(x-\xi)\} \sum_{n=0}^{\infty} \exp(-\beta_n(\alpha)|z|) \frac{1}{\lambda M_{-\infty}^2(\eta)} Y_n(\eta;\alpha)\, Y_n(y;\alpha)\, d\alpha \\ &= -\operatorname{sgn} z \int_{-\frac{1}{2}}^{\frac{1}{2}} d\xi \int_0^\infty \cos\{\alpha(x-\xi)\} \sum_{n=0}^{\infty} \exp(-\beta_n(\alpha)|z|)\, F_n(\xi;\alpha)\, Y_n(y;\alpha)\, d\alpha, \end{aligned} \tag{D 4}$$

where $F_n(\xi;\alpha)$ is defined by (11).

Then an expression for the cascade in figure 1 can be constructed from infinite summation in the form (6).

Appendix E. Consideration of the effect of the blade thickness

Let a blade profile $z = z_0(x,y)$ be given by

$$\partial z_0/\partial x = f(x,y) \pm \tfrac{1}{2} g(x,y),$$

where $g(x,y)$ denotes the contribution of thickness part to the slope of the blade surface. The fact that the effect of blade thickness is equivalent to that of pressure dipoles with axes parallel to the main flow suggests to us that the disturbance pressure p_τ due to the thickness contribution is represented by

$$\begin{aligned} p_\tau = -\sum_{m=-\infty}^{\infty} \int_{-\frac{1}{2}}^{\frac{1}{2}} d\xi \int_0^\infty \sin\{\alpha(x-\xi-mt\sin\gamma)\} \\ \times \sum_{n=0}^{\infty} \exp(-\beta_n(\alpha)|z-mt\cos\gamma|) \frac{\alpha}{\beta_n(\alpha)} G_n(\xi;\alpha)\, Y_n(y;\alpha)\, d\alpha. \end{aligned} \tag{E 1}$$

Then, the z-component of the velocity induced by the thickness effect is expressed at $z = 0$ as

$$\begin{aligned} \left[\frac{w}{U}\right]_{z=\pm 0} &= \pm \frac{1}{\kappa p_{-\infty} M_{-\infty}^2} \int_{-\frac{1}{2}}^{\frac{1}{2}} d\xi \int_0^\infty \cos\alpha(x-\xi) \sum_{n=0}^{\infty} G_n(\xi;\alpha)\, Y_n(y;\alpha)\, d\alpha \\ &\quad - \frac{1}{\kappa p_{-\infty} M_{-\infty}^2} \int_{-\frac{1}{2}}^{\frac{1}{2}} d\xi \int_0^\infty \sin\alpha(x-\xi) \sum_{n=0}^{\infty} S_n(\alpha)\, G_n(\xi;\alpha)\, Y_n(y;\alpha)\, d\alpha. \end{aligned} \tag{E 2}$$

from which it is known that $G_n(x;\alpha)$ is associated with $g(x,y)$ by

$$\left.\begin{aligned} \tfrac{1}{2}g(x,y) &= \frac{\pi}{\kappa p_{-\infty} M_{-\infty}^2} \sum_{n=0}^{\infty} G_n(x;\alpha)\, Y_n(y;\alpha) \\ \text{and hence} \qquad G_n(x;\alpha) &= \frac{\kappa p_{-\infty}}{2\pi} \frac{1}{\lambda} \int_0^{\lambda} g(x,y)\, Y_n(y;\alpha)\, dy. \end{aligned}\right\} \tag{E 3}$$

It should be noted that the first term on the right-hand side of (E 2) is the contribution of the blade at $z = 0$ and the second term is that of the other blades in the cascade. The effect of the second term which contributes to changing incidence angle must be taken into consideration, when $F_n(x;\alpha)$, i.e. the strength of the pressure dipoles with axes normal to the main flow which are associated with the camber and the angle of attack, is determined from the tangency condition on the blade mean camber surface corresponding to the boundary condition (5). More detailed study on the evaluation of the thickness effect is left to future research.

REFERENCES

HONDA, M. 1960 *Proc. Roy. Soc.* A **264**, 372.

HONDA, M. 1961 *Proc. Roy. Soc.* A **265**, 46.

NAMBA, M. & ASANUMA, T. 1965 *Trans. Japan Soc. Mech. Engrs* **31**, 1236 (in Japanese); *Bull. Inst. Space Aeron. Sci.* Univ. Tokyo, **1**, 164 (in Japanese).

NAMBA, M. & ASANUMA, T. 1967 *Bull. Japan Soc. Mech. Engrs* **10**, 920; *Rep. of Inst. Space Aeron. Sci.* Univ. Tokyo, **32**, 133.

SCHLICHTING, H. 1955 *VDI-Forsch-h.* 447.

SCHOLZ, N. 1950 *Ing.-Arch.* **18**, 84.

WARD, G. N. 1955 *Linearized Theory of Steady High-Speed Flow.* Cambridge University Press.

WATSON, G. N. 1944 *Theory of Bessel Functions,* 2nd ed. Cambridge University Press.